STRAIGHT SECTION IN SCALING FFAG ACCELERATOR

J.B. Lagrange*, Y. Mori, Kyoto University Research Reactor Institute, Kumatori, JAPAN

Abstract

Fixed Field Alternating Gradient (FFAG) synchrotrons are designed only in a circular shape, but straight sections can also be created. To keep the scaling condition, the field law in straight lines has to be different from the one in circular ring elements. These straight sections can be used for transport lines or insertions in FFAG rings like dispersion suppressors, leading to a new concept of advanced scaling FFAG.

INTRODUCTION

The concept of FFAG is usually applied to circular machines. In consequence, each cell is designed to provide a total bending angle. Based on previous studies [1, 2], the aim of this paper is to show how scaling FFAG unit-cells can also be created to guide particles with no overall bend. The scaling condition, i.e. a same phase advance per cell at every energy, leads to a different field law than in circular ring elements. This is the purpose of the first section. In the following sections, applications of these elements will be discussed, such as transport lines and insertions in FFAG rings.

FIELD LAWS IN SCALING FFAG

To determine the field law in scaling FFAG, we start from the transverse linearized equation of motion:

$$\frac{d^2Y}{ds^2} + K_Y Y = 0, \tag{1}$$

where s is the distance along the reference trajectory, and Y the transverse coordinate, i.e. x (horizontal) or z (vertical). K_x and K_z are given by

$$\begin{cases} K_x = \frac{1}{\rho^2} - K \\ K_z = K \end{cases}, \tag{2}$$

where ρ is the local curvature radius. K is the normalized gradient and is defined as $K = \frac{1}{B\rho}\left(\frac{\partial B_z}{\partial x}\right)_{z=0}$ with B the magnetic field and x the distance to the reference trajectory.

To obtain the field law in the circular elements, we make the following hypothesis: the approximation of small angles is used, so we consider $s \approx r\theta$ and $ds \approx rd\theta$, with notations given in Fig. 1. Indeed, we liken $s = \rho\xi$ to the distance $[AB]$:

$$[AB] = \rho \sin\xi = r \sin\theta \approx \rho\xi \approx r\theta. \tag{3}$$

We use cylindrical coordinates(r, θ, z).

In straight section elements, like in circular elements, we assimilate $s = \rho\xi$ to the distance $[AB]$:

$$[AB] = \rho \sin\xi = y \approx \rho\xi, \tag{4}$$

so $s \approx y$ and $ds \approx dy$. We use cartesian coordinates (x, y, z).

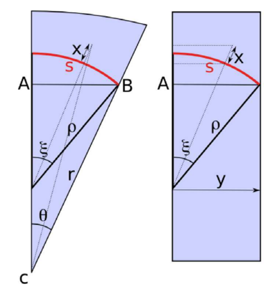

Figure 1: difference of geometry in circular ring element (left) and in straight section element (right).

With these hypothesis, we can derive Eq. 1 in both cases.

Circular Ring Element Case

With the circular element hypothesis, Eq. 1 becomes

$$\begin{cases} \frac{d^2x}{d\theta^2} + \frac{r^2}{\rho^2}(1 - K\rho^2)x = 0 \\ \frac{d^2z}{d\theta^2} + \frac{r^2}{\rho^2}(K\rho^2)z = 0 \end{cases} \tag{5}$$

The scaling condition sets that the equations of motion 5 are independent of momentum. Then,

$$\begin{cases} \frac{d\left(\frac{r^2}{\rho^2}\right)}{dP} = 0 \\ \frac{d(K\rho^2)}{dP} = 0 \end{cases} \Leftrightarrow \begin{cases} r \propto \rho \\ \frac{r}{B}\left(\frac{\partial B_z}{\partial x}\right)_{z=0} = k \end{cases} \tag{6}$$

with k the geometrical field index, independent of momentum. $r \propto \rho$ gives the geometrical similarity. Then, considering $x = r - r_0$ and $dx = dr$, we can integrate the differential equation of the system 6 in r. It leads to a unique solution:

$$B_z = B_0 \left(\frac{r}{r_0}\right)^k \tag{7}$$

with $B(r_0) = B_0$.

Straight Section Element Case

With the straight element hypothesis, Eq. 1 becomes

* lagrange@rri.kyoto-u.ac.jp

$$\begin{cases} \frac{d^2x}{dy^2} + \frac{1}{\rho^2}(1 - K\rho^2)x = 0 \\ \frac{d^2z}{dy^2} + \frac{1}{\rho^2}(K\rho^2)z = 0 \end{cases} \tag{8}$$

The scaling condition sets that the equations of motion 8 are independent of momentum. Then,

$$\begin{cases} \frac{d\left(\frac{1}{\rho^2}\right)}{dP} = 0 \\ \frac{d(K\rho^2)}{dP} = 0 \end{cases} \Leftrightarrow \begin{cases} \rho = const. \\ \frac{1}{B}\left(\frac{\partial B_z}{\partial x}\right)_{z=0} = \frac{n}{\rho} \end{cases} \tag{9}$$

where n is now the field index, also independent of momentum. $\rho = const.$ gives the geometrical similarity. Then, considering $x = X$ and $dx = dX$, with X the transverse cartesian coordinate, we can integrate the differential equation of the system 9 in X. It leads to a unique solution [3]:

$$B_z = B_0 e^{\frac{n}{\rho}(X - X_0)} \tag{10}$$

with $B(X_0) = B_0$.

Bending Section Element Case with an infinite radius

Another point of view to get the law in straight sections would be to see them as circular sections with an infinite radius. FFAG straight sections have been studied [4] with a field law in $\left(\frac{x}{x_0}\right)^k$, and this approximation gives the same result if x_o is infinite. Indeed, if r_0 tends to the infinite:

$$\lim_{r_0\to\infty}\left(\frac{r}{r_0}\right)^k = \lim_{r_0\to\infty}\left[\left(1 + \frac{x}{r_0}\right)^{\frac{r_0}{x}}\right]^{\frac{x}{r_0}k} \tag{11}$$

with $r = x + r_0$.
k in circular elements is the geometrical field index, and not strictly speaking the field index : $k = \frac{r_0}{\rho}n$, n being the field index. So we get back to the exponential law [5]:

$$\begin{aligned} \lim_{r_0\to\infty}\left(\frac{r}{r_0}\right)^k &= \left[\lim_{r_0\to\infty}\left(1 + \frac{x}{r_0}\right)^{\frac{r_0}{x}}\right]^{\frac{n}{\rho}x} \\ &= e^{\frac{n}{\rho}x} \end{aligned} \tag{12}$$

TRANSPORT LINE

To confirm the exponential field law in straight sections, stepwise tracking using Runge Kutta integration in hard edge field has been realized. An example with a unit-cell made up of two rectangular magnets, one focusing, the other defocusing, has been designed. In this case, particles are protons. We start in the middle of a magnet, to enter in the unit-cell with no angle. Reference trajectories are obtained and plotted in Fig. 2. Phase advances are obtained from Fast Fourier Transform (FFT) analysis, tracking the particle 1024 times through the cell with small initial amplitude (1 mm). As expected, both horizontal and vertical phases advance are constant: $\mu_x = 104.8\ deg.$ in horizontal and $\mu_z = 112.5\ deg.$ in vertical.

Table 1: Tracking parameters

Length of the magnets	60 cm
Drift	40 cm
Kinetic energy range	80 to 200 MeV
Field index	17
Local curvature radius	2.1 m
Step size	1 mm
Phase advances:	
horizontal μ_x	104.8 deg.
vertical μ_z	112.5 deg.

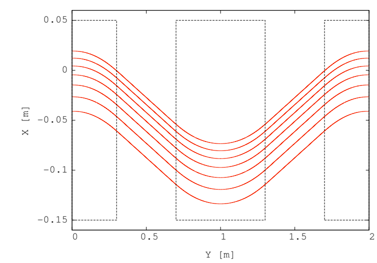

Figure 2: reference trajectories for kinetic energies from 80 MeV (bottom) to 200 MeV (up).

INSERTIONS

Matching of reference trajectories

Straight sections could be used with bending FFAG sections, but since field laws in each section are different, it will occur a difference of reference trajectories at the border. The purpose of this chapter is to deal with the matching of these different reference trajectories.

If we match the different cells for a special momentum P_m, then the condition of matching for the other momenta will be

$$\left(1 + \frac{x - r_m}{r_m}\right)^{k_{circ.}+1} = e^{\frac{n_{str.}}{\rho_{str.}}(x - r_m)} \tag{13}$$

with $k_{circ.}$ the geometrical field index and r_m the average radius of a particle with a momentum P_m in circular section. $n_{str.}$ and $\rho_{str.}$ are respectively the field index and the local curvature radius in straight section. Eq. 13 can be solved to the first order:

$$\frac{n_{str.}}{\rho_{str.}} = \frac{k_{circ.} + 1}{r_m} \tag{14}$$

The effects of higher orders create a reference trajectories mismatch for momenta other than P_m. By choosing this particular momentum, the maximum mismatch could be minimized. An example has been computed by inserting straight sections in the 150 MeV FFAG ring built in KEK [6], for kinetic energies between 20 MeV and 150 MeV. The result of reference trajectories mismatch between circular parts and straight parts appears on Fig. 3. This maximum mismatch is around 1 cm for this case, but it would be smaller for larger rings. All things being equal, the more $k_{circ.}$, the smaller the reference trajectory mismatch.

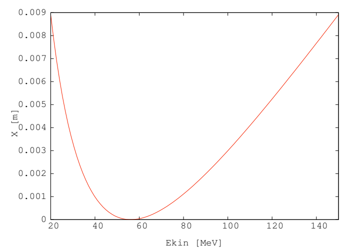

Figure 3: difference of reference trajectories between circular cells and straight cells in 150 MeV FFAG ring example.

Dispersion Suppressor

In FFAGs, since every energy has a different reference trajectory, dispersion suppressors can be useful in applications where all energies are needed at the same position, such as at the end of a transport line [4], or where excursion is larger than RF cavities in FFAG rings [7]. The purpose of this chapter is to study a possibility of dispersion suppressors in straight sections.

The effect of a dispersion suppressor would be to suppress the excursion and bring every reference trajectory at the same point. In scaling straight FFAG cells, the excursion between 2 momenta P_0 and P_1 is generated from Eq. 10:

$$X_{tot.} = X_1 - X_0 = \frac{1}{n/\rho} ln\left(\frac{P_1}{P_0}\right) \qquad (15)$$

One principle of a dispersion suppressor would be to increase the factor n/ρ of the exponential law in the cells, to create a transverse difference of the reference trajectories, centered on the matched momentum P_0. This difference x for a momentum P_1 is given by

$$x = ln\left(\frac{P_1}{P_0}\right)\left(\frac{\rho_0}{n_0} - \frac{\rho_1}{n_1}\right) \qquad (16)$$

with n_0/ρ_0 the factor of the normal cell, and n_1/ρ_1 the factor of dispersion suppressor.

This difference excites a betatron oscillation of the beam, and distort the reference trajectory. If the cell has 180-degree phase advance, the total reduction of excursion is twice the difference of the reference trajectories.

This assumption is valid only for small differences of reference trajectories, and several cells are necessary to suppress a large excursion. If the reduction of excursion is kept constant for every 180-degree phase advance cell, the total number of cells N is determined by

$$N = \frac{n_1/\rho_1}{2\,(n_1/\rho_1 - n_0/\rho_0)} \qquad (17)$$

with n_0/ρ_0 the factor of the normal cell, and n_1/ρ_1 the factor of the first cell of the dispersion suppressor.

If the dispersion suppressor is made up of $N = 1$ cell, the factor n_1/ρ_1 of the dispersion suppressor cell is twice n_0/ρ_0 of the normal cells.

A scheme of a dispersion suppressor with $N = 2$ cells appears on Fig. 4. In this case, $(n/\rho)_{cell1} = \frac{4}{3}\,(n/\rho)_{normal}$ and $(n/\rho)_{cell2} = 4\,(n/\rho)_{normal}$.

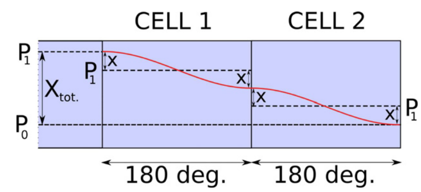

Figure 4: Dispersion suppressor made of 2 cells with 180-degree phase advance each. Doted lines show intrinsic reference trajectories of the cells, and red line shows the distortion of reference trajectories generated by the difference x.

After dispersion suppressors, since all energies are at the same position, no focusing effect is feasible with keeping the zero-dispersion condition. In cases where a small dispersion is sufficient but on long distances [7], it would worth to just reduce the dispersion instead of suppressing it, to keep the possibility of focusing the particles.

Dispersion suppressors can also be imagined in circular sections.

SUMMARY

Straight sections in scaling FFAGs can be designed with a transverse exponential magnetic field law. Tracking in geometrical model of field has been done to confirm this scaling law. Applications such as transport lines and insertions in FFAG rings can be imagined. Some of them imply to connect these straight sections with bending sections, so to deal with the difference of reference trajectories that issues from it. However this difference can be minimize. Another point has been highlighted: dispersion suppressors in straight sections. A principle has been proposed.

REFERENCES

[1] P.F. Meads Jr, “A dispersion-free long straight section for a fixed-field alternating-gradient synchrotron”, IEEE Trans. Nucl. Sci. NS-22, 2448 (1983).

[2] P.F. Meads Jr, “A Compensated Dispersion-free Long Insertion for an FFAG Synchrotron”, PAC’93.

[3] T. Planche, private communication.

[4] S. Machida, “Beam transport line with scaling fixed field alternating gradient type magnets”, about to be published.

[5] T. Uesugi, private communication.

[6] M. Aiba et al., “A 150 MeV FFAG with return-yoke free magnet”, Proceedings of PAC01.

[7] T. Planche and Y. Mori, “Harmonic number jump acceleration in scaling FFAG ring”, PAC’09.